ACTA ABP BIOCHIMICA POLONICA

Vol. 59, No 4/2012
653–660
on-line at: www.actabp.pl

Regular paper

Assessment of the free binding energy of 1,25-dihydroxyvitamin D_3 and its analogs with the human VDR receptor model

Karol Kamel✉ and Andrzej Kolinski

Laboratory of Theory of Biopolymers, Faculty of Chemistry, University of Warsaw, Warsaw, Poland

1,25-dihydroxyvitamin D_3 has quite significant anticancer properties, but its strong calcemic effect in principle excludes it as a potential anticancer drug. Currently, a lot of effort is being devoted to develop potent anticancer analogs of 1,25-dihydroxyvitamin D_3 that would not induce hypercalcemia during therapy. In this work, the free binding energy of the VDR receptor with 1,25-dihydroxyvitamin D_3 and its three potent analogs (EB 1089, KH 1060 and RO 25-9022) is calculated and compared with each other. With this approach, we could estimate the relative binding affinity of the most potent analog, RO 25-9022, and also revealed a quite distinct mechanism of its interaction with VDR.

Key words: vitamin D, docking, drug design, KH 1060, RO 25-9022, EB 1089

Received: 28 June, 2012; revised: 21 September, 2012; accepted: 04 October, 2012; available on-line: 16 October, 2012

INTRODUCTION

Vitamins D are a group of lipid-soluble organic compounds causing a variety of physiological responses. The most important vitamins of the vitamin D group are vitamin D_2 (ergocalciferol) produced by plankton and fungi from ergosterol and vitamin D_3 (cholecalciferol) produced by animals and humans from 7-dehydrocholesterol. Both compounds are synthesized when an organism is exposed to UV radiation (Holick, 2008). Vitamin D_3 is biologically inactive; it undergoes hydroxylation at the C25 position and conversion to prohormone calcidiol (25-hydroxycholecalciferol) in the liver, and, subsequently, hydroxylation at the 1αC position and conversion in kidneys to calcitriol (1,25-dihydroxycholecalciferol or $1,25(OH)_2D_3$) (Guyton *et al.*, 2003), a biologically active form of vitamin D_3. The extent of biological activities of vitamin D is remarkable. The biological functions of vitamin D we are currently aware of include regulation of the intestinal absorption of calcium and phosphates (Meyer *et al.*, 2006; Barthel *et al.*, 2007), autoimmune disease prevention (Cantorna *et al.*, 1996; Zella & DeLuca, 2003; Cantorna & Mahon, 2004), osteoclastogenesis and mineralization of bones (Fretz *et al.*, 2006; Milat & Ng, 2009; Haussler *et al.*, 2010), antiproliferative activity and prevention of prostate cancer (Zhuang & Burnstein, 1998; Boyle *et al.*, 2001; Moffatt *et al.*, 2001), breast cancer (James *et al.*, 1996; Narvaez *et al.*, 1997; Wu *et al.*, 1997; Malinen *et al.*, 2008), colon cancer (Evans *et al.*, 1999; Gaschott *et al.*, 2001), pancreatic cancer (Kawa *et al.*, 1997; Schwartz *et al.*, 2008; Chiang *et al.*, 2009) and ovarian cancer (Li *et al.*, 2004), mainly through the regulation of the expression of cyclin-dependent kinase inhibitors (p21 and p27), and it seems to be a good candidate for anticancer therapies (Nickeleit *et al.*, 2007). $1,25(OH)_2D_3$ bioactivity involves mainly binding with the vitamin D receptor (VDR) (Rochel *et al.*, 2000). The VDR molecule has two binding sites for the $1,25(OH)_2D_3$ molecule: the main (genomic) binding site responsible for the regulation of transcription of various genes and indirectly for the biological effects mentioned above, and an additional (alternative) binding site responsible for the "rapid response", because certain specific biological effects can appear after 1–2 minutes. $1,25(OH)_2D_3$ binding to the genomic site occurs in the VDR molecule localized in the nucleus, whereas binding to the alternative pocket usually occurs in the caveolae (Haussler *et al.*, 2011).

Such a significant role of $1,25(OH)_2D_3$ in the human body drew attention of many research groups which initiated projects toward the ultimate goal: design and synthesis of new, potent and selective 1,25-dihydroxyvitamin D_3 analogs (Brown & Slatopolsky, 2008). It is especially promising as novel anticancer compounds are at hand, although the mechanism by which various $1,25(OH)_2D_3$ analogs elicit specific responses is yet unknown (Singarapu *et al.*, 2011).

In this paper, the binding energies of $1,25(OH)_2D_3$ and selective and potent VDR agonists with significant anticancer properties (Leo Pharma EB 1089, Leo Pharma KH 1060 and Hoffmann-La Roche RO 25-9022, being one of the most bioactive $1,25(OH)_2D_3$ analogs in terms of the stimulation of cellular differentiation and inhibition of cellular proliferation) (Uskokovic *et al.*, 2001; van den Bemd & Chang, 2002; Guyton *et al.*, 2003; Fig. 1) to the genomic binding site of reduced VDR (redVDR) were assessed and compared with one another.

MATERIALS AND METHODS

Crystallographic structures of the published VDR/ligand complexes are characterized by the almost identical conformation of the ligand binding domain (genomic site) (Rochel *et al.*, 2000; Tocchini-Valentini *et al.*, 2001; 2004; Singarapu *et al.*, 2011). The structures of the reduced VDR receptor and of $1,25(OH)_2D_3$ were constructed on the basis of the crystallographic structure of $1,25(OH)_2D_3$/VDR (PDB entry: 1DB1). The remaining ligand structures were built on the basis of the $1,25(OH)_2D_3$ structure with a conserved *trans* configura-

✉e-mail: kamel@chem.uw.edu.pl

Abbreviations: PDB, Protein Data Bank; 1,25(OH)2D3, 1,25-dihydroxycholecalciferol; EB 1089, 1,25-dihydroxy-24,26,27-trishomo-22E,24E-diene-cholecalciferol; KH 1060, 1,25-dihydroxy-20-epi-22-oxa-24,26,27-trishomo-cholecalciferol; RO 25-9022, 1,25-dihydroxy-16,23E-diene-26,27-hexafluoro-19-nor-cholecalciferol

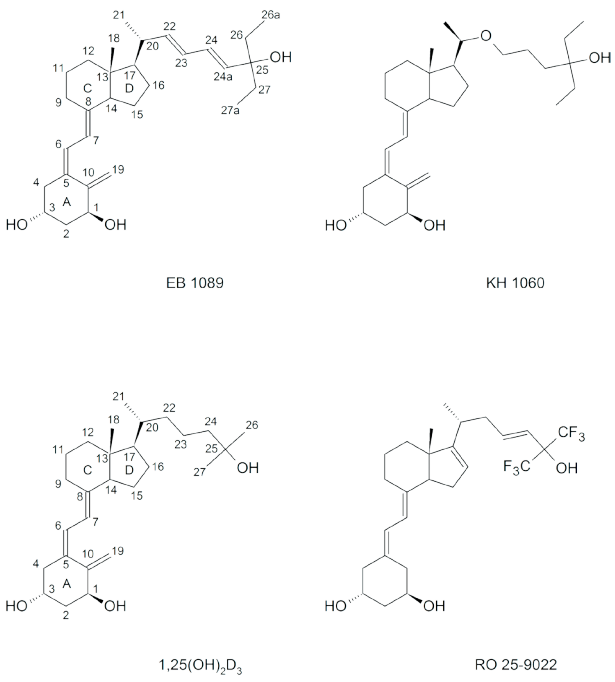

Figure 1. Numbering of $1,25(OH)_2D_3$ and related structural analogs.

tion of the C6-C7 bond, conformation of the cyclohexane ring (A-ring), octahydroindene ring (C,D-rings) and the angle between the ring planes of 30° (Rochel *et al.*, 2000; Haussler *et al.*, 2011). The redVDR model was constructed using the following amino acids from the 1DB1 structure: Tyr143-Lys240, Ala267-Lys322, Leu393-Gly423 (Fig. 2). The addition of hydrogen atoms to ligands and redVDR was carried out using the Chimera program (Pettersen *et al.*, 2004). Ionizable amino acid residues were protonated according to physiological (cellular) pH. The structures of ligands and redVDR were parameterized with Gasteiger atomic partial charges using Chimera. The molecular docking procedure was performed using Auto Dock software (Morris *et al.*, 1998). The docking procedure was as follows: the ligands were docked inside a cuboid grid box with a spacing of 0.375 Å and dimensions of 19.5 × 19.5 × 14.25 Å which allowed sampling actual ligand-accessible regions. A Lamarckian genetic algorithm was used for 2.5×10^6 energy evaluations for each of 100 docking trials. To obtain the docked conformations of $1,25(OH)_2D_3$ and analogs, clustering at 0.5 Å was performed. The docking procedure used was a semi-flexible method which means that redVDR was treated as a rigid molecule and $1,25(OH)_2D_3$ and analogs had flexible torsion angles. During the docking procedure, the torsion angles C4-C3-O-H, C10-C1-O-H, C16-C17-C20-C22, C17-C20-C22-C23, C20-C22-C23-C24, C22-C23-C24-C25, C23-C24-C25-O and C24-C25-O-H were subject to change. In the calcitriol analogs, the torsion angles allowed to change were the same as in 1,25-dihydroxyvitamin D_3 with the exclusion of angles containing double bonds or a conjugated bonds system. Additionally, in EB 1089 and KH 1060, the rotational freedom of ethyl groups was taken into account.

Table 1 contains binding energies (Auto Dock score), RMS values and hydrogen bond parameters for the docked structures of $1,25(OH)_2D_3$ and analogs.

In the second part of our calculations a rescoring protocol based on a method developed by Fanfrlík *et al.* (2010) was employed as the results of calculations using this method were found to be consistent with known experimental data. Moreover, we used this protocol earlier to propose a novel binding mode of epothilone A to β-tubulin (Kamel & Kolinski, 2011).

To generate a ligand conformation that corresponds to the "global" potential energy minimum, a molecular dynamics (MD) method was used for $1,25(OH)_2D_3$ and the analogs. MD simulations were run using the AMBER force-field (Cornell *et al.* 1995) at a constant temperature of 1000 K using the Andersen thermostat. Equilibration time was 5 ps and production run was 10 ps. One-hundred resulting structures were generated for each ligand. Subsequently, the ligand/redVDR complexes and the redVDR molecule were geometrically optimized in a COSMO continuous solvent model (Klamt & Schuurmann, 1993) and in the gas phase using a PM6 semiempirical quantum mechanics method (Stewart, 2007) with dispersion and hydrogen bond corrections (PM6-DH2, Korth *et al.*, 2010) with the MOZYME module (Stewart, 2009) using localized molecular orbitals implemented in MOPAC2009 (Stewart, 2008). The resulting structures from docking and MD were geometrically optimized using the PM6-DH2 method in continuous solvent. Apart from this methodology, an alternative approach was also attempted, which was a direct geometry optimization of ligand structures built on the basis of $1,25(OH)_2D_3$. Such an approach was based on the fact that the backbone of all the ligands was almost identical,

Table 1. Energy and structural parameters for docked conformations of $1,25(OH)_2D_3$ and analogs.
Auto Dock binding energies (score, *E*, kcal/mol), hydrogen bond parameters (Å, deg) and RMS values (Å) between corresponding experimental and docked structures. RMS1 was calculated on heavy atoms. RMS2 is RMS1 with positional correction (rotation and translation were taken into account).

Molecule	$1,25(OH)_2D_3$	EB 1089	KH 1060	RO 25-9022
E	–17.7	–17.5	–17.8	–16.2
RMS1	0.46	0.78	0.71	–
RMS2	0.56	0.96	0.85	–
O25···H–N–His397	2.00; 161.7	–	1.86; 175.4	1.72; 166.2
O25–H···N–His305	2.07; 139.8	2.28; 168.7	1.99; 145.0	1.86; 136.5
O1–H···O–Ser237	1.93; 133.5	1.97; 143.9	1.89; 149.4	1.95; 126.5
O1···H–N–Arg274	1.87; 170.8	1.67; 166.8	1.87; 173.8	1.72; 163.5
O3···H–O–Ser278	1.78; 132.3	1.94; 117.7	1.77; 130.3	1.91; 130.0
O3···H–O–Tyr143	2.07; 167.6	1.88; 157.7	2.05; 166.4	1.91; 168.5

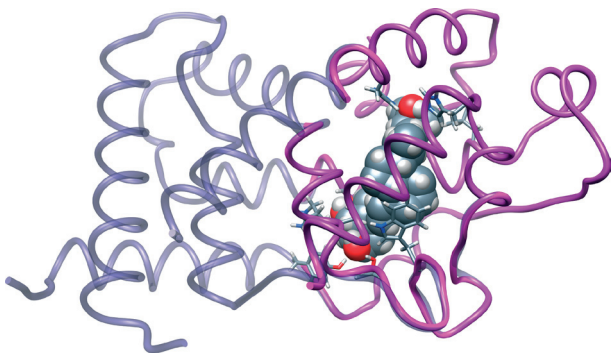

Figure 2. Superposition of human vitamin D receptor (gray, transparent) and reduced vitamin D receptor models (magenta, opaque).
Sphere representation of $1,25(OH)_2D_3$ bound to VDR with stick representation of interacting amino acids.

and the differences in the side chain would not significantly affect ligand deformation energy.

In this part of the work, our aim was to calculate the free binding energy of $1,25(OH)_2D_3$ and analogs with the redVDR molecule. We adopted an approach based on the thermodynamic cycle proposed by Raha and Merz (2005):

$$\Delta G^{w}_{bind} \approx \Delta G_{int} + [[\Delta H_f^{w}(PL) - \Delta H_f(PL)] - [\Delta H_f^{w}(P) - \Delta H_f(P)] - [\Delta H_f^{w}(L) - \Delta H_f(L)] - [\Delta H_f(P) - \Delta H_f^{complex}(P)] - [\Delta H_f(L) - \Delta H_f^{complex}(L)]]. \quad (1)$$

$$\Delta G_{int} = \Delta H_{int} - T\Delta S. \quad (2)$$

$$\Delta H_{int} = \Delta H_f(PL) - [\Delta H_f^{complex}(P) + \Delta H_f^{complex}(L)]. \quad (3)$$

ΔG^{w}_{bind} is the estimated free binding energy in the water environment, $\Delta H_f^{w}(X)$ is the heat of formation in aqueous solution, where X stands for the free protein, free ligand or protein-ligand complex. Likewise, $\Delta H_f(X)$ are the heats of formation in the gas phase of the free ligand, free protein or protein-ligand complex. $\Delta H_f^{complex}(X)$ is the enthalpy of the ligand or the protein molecule in the complex conformation. ΔG_{int} is the interaction energy in the gas phase. Heats of desolvation and deformation are:

$$\Delta G_c = [\Delta H_f^{w}(X) - \Delta H_f(X)] - [\Delta H_f(X) - \Delta H_f^{complex}(X)]. \quad (4)$$

X stands for the ligand or protein molecule. All heats of formation were calculated at 298 K. Entropy changes (ΔS) were calculated *in vacuo* using the AMBER forcefield.

RESULTS AND DISCUSSION

The molecular docking of the 1,25-dihydroxyvitamin D_3 molecule its and analogs to redVDR generated complexes very similar to corresponding crystallographic structures. For the $1,25(OH)_2D_3$/redVDR complex all hydrogen bonds present in the crystallographic structure were reconstructed (see Fig. 3A, Table 1). The hydrogen bonding pattern observed in the remaining crystallographic structures was also reconstructed (Fig. 3B). The most important contacts defining bioactivity are O1-H hydrogen bonds with Ser237 and Arg274, and O25-H with His397 and His305. An exception to the rule is the EB 1089/redVDR complex in which the O25···H-N-His397 hydrogen bond was broken, but the polar contact was maintained (3.62 Å). This effect could be attributed to the high rigidity of the conjugated bonds system between C22-C23 and C24-C24a

Table 2. Ligand side chain/receptor interactions observed in $1,25(OH)_2D_3$, EB 1089, KH 1060 and RO 25-9022/redVDR complexes.

Residue	Atom	$1,25(OH)_2D_3$	EB 1089	KH 1060	RO 25-9022
Leu227	CD1	C26(3.65)	C26(3.57) C26a(2.93)	C26(3.05) C26a(3.02)	C26(3.56)
Ala231	N	C26(4.00)	C26(3.52)	C26a(3.81)	–
Val234	CG1	C27(3.97)	C27a(3.58)	C27a(3.47)	C27(3.71)
	CG2	C24(3.43)	–	C24a(3.43)	–
Val418	CG1	C27(3.89)	–	C27a(3.68)	–
Phe422	CE1	C27(3.98)	C27a(3.38)	C27a(3.72)	–
	CD1	–	C27a(3.84)	–	–
His305	CD2	C23(3.94)	–	C23(3.65)	C23(3.63) C22(3.92)
	NE2	C23(3.63)	C24a(3.58)	C23(3.98)	C24(4.00) C23(3.46)
Val300	CG1	C21(3.98)	–	O22(3.54)	–
Leu309	CD2	C21(3.65)	–	C21(3.70)	–
Leu230	CB	–	C26(3.52) C26a(3.26)	C26a(3.05)	–
	CD1	–	C26a(3.91)	–	–
Ala303	CB	–	C26a(3.46)	–	–
His397	NE2	–	C24a(3.89)	–	–
	CD2	–	–	–	C21(3.86)
Ile268	CD1	–	C21(3.78)	–	–
Met272	CE	–	C21(3.46)	–	–

Table 3. Ligand side chain/receptor interactions observed in $1,25(OH)_2D_3$, EB 1089, KH 1060 and RO 25–9022/redVDR PM6–DH2 optimized complexes.

Residue	Atom	$1,25(OH)_2D_3$	EB 1089	KH 1060	RO 25–9022
Leu227	CD1	C26(3.42)	C26(3.55) C26a(3.33)	C26(3.49) C26a(3.42)	C26(3.77)
	O	–	–	C26a(3.27)	–
Ala231	N	C26(3.81)	C26(3.35)	C26a(3.29)	–
	CA	C26(3.75)	C26(3.28)	C26a(3.65) C27(3.77)	–
	CB	C26(3.91)	C26(3.62)	C26a(3.89)	–
Val234	CG1	C27(4.00) C24(3.84)	C27a(3.40)	C27a(3.41)	C27(3.92)
	CG2	C24(3.62) C23(3.80)	C24(3.54) C23(3.82)	C24a(3.59)	C24(3.99)
Val418	CG1	C27(3.43)	C27(3.42) C27a(3.64)	C27(3.80) C27a(3.47)	–
	CG2	–	C27a(3.98)	C27a(3.85)	–
Phe422	CE1	C27(3.75)	C27a(3.43)	C27a(3.41)	C27(3.83)
	CD1	C27(3.72)	C27a(3.44)	C27a(3.40)	C27(3.75)
His305	CD2	C23(3.79) C21(3.62)	C22(3.99)	C24(3.72) C23(3.38)	C23(3.40) C22(3.81)
	NE2	C23(3.44) C21(3.87)	C24a(3.13) C24(3.84) C22(3.85)	C26(3.82) C24(3.34) C23(3.60)	C24(3.76) C23(3.23)
	CE1	–	C24a(3.71)	–	–
Val300	CG1	C21(3.62) C20(3.92)	C20(3.94)	C23(3.90) O22(3.35) C21(3.54) C20(3.90)	C21(3.97) C20(3.56)
Leu309	CD2	C21(3.47)	C21(3.60)	C21(3.46)	C21(3.56)
Leu230	CB	–	C26a(3.68)	C26a(3.67)	–
	CD1	–	C26a(3.91)	–	–
	O	–	C26(3.69)	C26a(3.82)	–
	C	–	C26(3.61)	C26a(3.49)	–
Ala303	CB	–	C26a(3.32)	C26a(3.58) C23(3.80)	C22(3.97)
	O	–	C26a(3.23)	C26(3.28) C26a(3.67)	–
His397	NE2	C24(3.52) C23(3.86)	C24a(3.29) C24(3.82) C23(3.69)	C27a(3.70) C24a(3.69) C24(3.43)	C23(3.92)
	CD2	–	C23(3.98)	C24(3.66)	C21(3.96)
	CE1	–	C27a(3.95)	C27a(3.91)	
Ile268	CD1	–	C23(3.68)	–	–
Met272	CE	–	C21(3.67)	–	–
Tyr401	CD1	C27(3.59)	C27(3.66)	C27a(3.72)	–
	CE1	C27(3.52)	C27(3.55)	C27a(3.71)	–
Leu414	CD2	C26(3.91) C27(3.95)	C27(3.49)	C27(3.79)	C26(3.92)
Leu313	CD1	C21(3.78)	C21(3.40)	C21(3.37)	C21(3.82)
Leu404	CD2	C26(3.97)	–	C26(3.61)	–

and the longer side chain compared to $1,25(OH)_2D_3$. For the RO 25-9022/redVDR complex, the reconstruction of hydrogen bonds formed by O25-H with His397 and His305 and O1-H with Ser237 and Arg274 was rather unsurprising, as the RO 25-9022 side chain was of equal length to the $1,25(OH)_2D_3$ side chain and had only one double bond at C23, which did not impair its flexibility in a significant way.

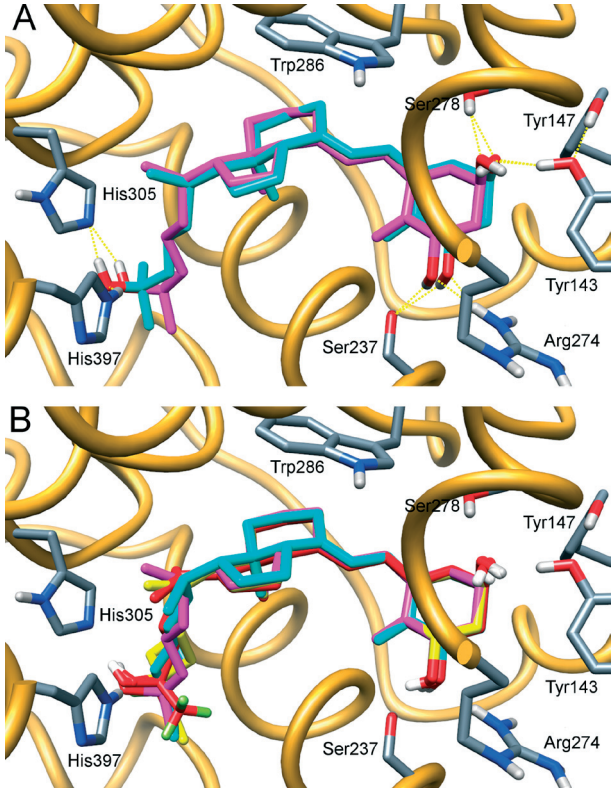

Figure 3. Genomic binding pocket of VDR.
Panel A shows a superposition of $1,25(OH)_2D_3$ molecules: conformation derived from the 1DB1 structure (cyan) and docked conformation (magenta). Yellow dashed lines represent hydrogen bond interactions between ligands and the receptor molecule. **Panel B** shows a superposition of docked structures of $1,25(OH)_2D_3$ (magenta), EB 1089 (cyan), KH 1060 (yellow) and RO 25-9022 (red).

The binding pocket of the vitamin D receptor consists of many hydrophobic residues capable of interacting with $1,25(OH)_2D_3$ and analogs through van der Waals forces. Since the conformation and position of the backbone fragment inside VDR are virtually identical for all the compounds, with a slight exception of RO 25-9022 which lacks the methylene group at C10, we focused mainly on the side chain/protein contacts. The side chain/protein aliphatic van der Waals contacts are listed in Table 2.

The geometry optimization procedure at the PM6-DH2 theory level resulted in an improvement and increased number of contacts between the ligand side chains and the receptor molecule, as expected (see Table 3). The van der Waals contacts with Leu227, Ala231, Val234, Val300, His305, Leu309, His397, Leu414, Val418 and Phe422 observed in experimental structures (Tocchini-Valentini *et al.*, 2004) were reconstructed.

It can be clearly seen from Table 3 that the number of aliphatic chain/protein contacts in PM6-DH2-optimized complexes increased considerably in comparison with the number of contacts in experimental and docked structures (Tocchini-Valentini *et al.*, 2004; Table 2). The main cause of this effect is probably the fact that the VDR crystallographic structures are always characterized by almost identical receptor molecule conformations, which in turn forces the almost identical ligand conformations. This is most probably due to the strong lateral contacts between VDR molecules and their packing that force the adoption of one, specific, geometrically favored conformation (Singarapu *et al.*, 2011). The geometrically optimized structures are not part of a crystal structure, so they are not subjected to strong lateral interactions generated by neighboring VDR molecules and therefore they retain their significant number of degrees of freedom and can interact with ligand molecules as in the induced-fit model. In this way, the interactions between redVDR and a ligand molecule resemble those found in real biological systems.

The O25-H hydrogen bonds are among the most important interactions responsible for the ligand bioactivity, as noted above (Vaisanen *et al.*, 2002). In the case of $1,25(OH)_2D_3$ and KH 1060 molecules, the length and angle of hydrogen bonds between O25-H and the two histidine imidazoles are very similar to each other, as clearly seen from Table 4. The length and rigidity of the side chain in the EB 1089 molecule places the O25-H hydroxyl group in a less favorable position, which weakens the O25−H···N−His305 hydrogen bond and severely disrupts the O25···H−N−His397 hydrogen bond (3.425 Å; 160.2°).

The analysis of the RO 25-9022/redVDR complex O25-H hydroxyl group hydrogen bonding yielded qualitatively different results from those obtained for the compounds discussed above. During both *in vacuo* and continuous water model geometry optimization procedures using the PM6-DH2 method and the MOZYME function, the O25 hydrogen was transferred to the His305 imidazole nitrogen (NE atom). The cause of this effect is the extraordinary electron withdrawing property of the trifluoromethyl group (Swain *et al.*, 1983).

Two simplified systems, each consisting of two histidine side chain fragments (from His305 and His397, respectively) and one of RO 25-9022 and one of the $1,25(OH)_2D_3$ side chain fragments (C23-C27) were built to obtain more quantitative results for this proton transfer effect. The systems were optimized using the PM6-DH2 method in the gas phase, in the continuous water environment and using a wide range of dielectric constants to simulate a protein interior environment (Schutz & Warshel, 2001). The analysis of geometry-optimized systems with the RO 25-9022 side chain fragment showed that proton transfer occurred for dielectric constant ≥ 4. Our preliminary calcula-

Table 4. O25-H hydrogen bond interactions in $1,25(OH)_2D_3$, EB 1089, KH 1060 and RO 25-9022/redVDR PM6-DH2 optimized complexes.

Molecule	$1,25(OH)_2D_3$	EB 1089	KH 1060	RO 25-9022
O25···H–N–His397	1.714;166.4	–	1.766;163.2	–
O25–H···N–His305	2.025;156.6	2.540;127.6	2.048,159.2	–
O25(-)···H–N–His397	–	–	–	1.662;174.1
O25(-)···H–N–His305	–	–	–	1.488;152.5

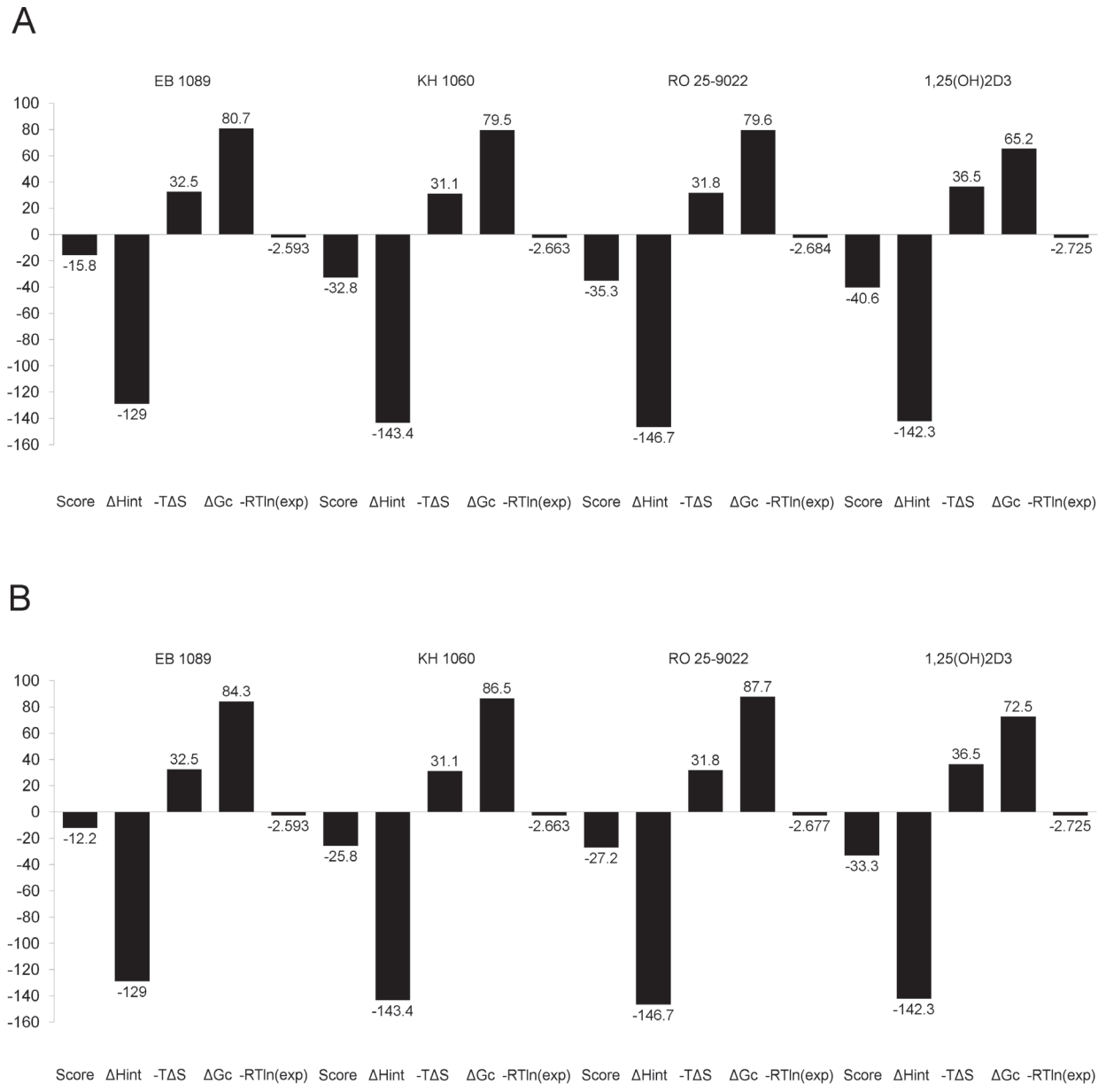

Figure 4. Total score and contributing terms for ligands/redVDR complexes.
Panel A shows scores from the ligand geometry optimization procedure. **Panel B** shows scores from the molecular dynamics/ligand geometry optimization procedure. ΔH_{int} — enthalpy of interaction *in vacuo*, $-T\Delta S$ — entropy term, ΔG_C — sum of desolvation and deformation enthalpies, $-RT\ln(exp)$ — binding free energy with respect to the relative experimental binding constants.

tions using the Density Functional Theory with a small basis set (3-21G), a hybrid three-parameter functional (B3LYP) and COSMO solvation model carried out in the GAMESS program (Schmidt *et al.*, 1993) showed similar results for dielectric constants ≥ 8. These findings correlate well with the dielectric constants applicable to protein interiors (Schutz & Warshel, 2001). It is obvious that such an effect was not observed in the system containing the $1,25(OH)_2D_3$ side chain fragment as the methyl groups at C25 have rather electron donating properties.

The analysis of the free binding energy (or rather the "score" as a direct comparison of the results obtained from isothermal titration calorimetry and this method is not possible due to the differences in construction of the scoring function (Fanfrlík *et al.,* 2010)) of $1,25(OH)_2D_3$ and analogs to redVDR yielded expected results consistent with experimental data. Our calculations clearly show that despite numerous side chain/protein contacts in the EB 1089/redVDR complex, its score has the least negative value that indicates the smallest binding affinity of this ligand (see Fig. 4), which is not very surprising given the weak hydrogen bond interactions of O25-H. $1,25(OH)_2D_3$ has the highest binding affinity (score) of all of the compounds investigated, which is due to the very flexible side chain that facilitates a significant number of side chain/protein interactions and permits the formation of strong hydrogen bonds at O25-H. The high score achieved by the KH 1060 molecule could clearly be attributed to the length and flexibility of its side chain that enabled most side chain/protein contacts of all the molecules under investigation and provided a conformation necessary for strong hydrogen

bonding between O25-H and His397 and His305, respectively. The higher score obtained by RO 25-9022 could in turn be attributed to the proton transfer effect which certainly strengthens the hydrogen bonds formed and accepted by O25-H through electrostatic interactions.

A comparison of the results of our binding free energy calculations with the data provided by Tocchini-Valentini *et al.* (2004) showed very good correlation. In Tocchini-Valentini *et al.* (2004), relative values of ligand/VDR binding affinity were given. The binding of $1,25(OH)_2D_3$ was assumed as 100, whereas the relative binding affinities of KH 1060 and EB 1089 were determined as 90 and 80, respectively. Assigning the scores obtained from the simple ligand geometry optimization procedure (Fig. 4A) to the respective values given by Tocchini-Valentini *et al.* (2004), using the -RTln(experimental % of binding) equation produced relative binding affinities. The same approach was applied for the scores obtained from the MD/ligand geometry optimization procedure. On the basis of these results, we can estimate the relative binding affinity of RO 25-9022 to be about 92-93.

CONCLUSIONS

The Auto Dock docking/PM6-DH2 rescoring procedure employed in this study generated results in good agreement with those obtained by Tocchini-Valentini *et al.* (2004), which clearly shows the usefulness of this methodology in assessing the free binding energy of various compounds.

The direct application of a semiempirical quantum mechanics method (PM6-DH2) allowed for more precise calculations of the heat of interactions than would be possible using the molecular mechanics methodology only and we could study subtle effects such as the proton transfer effect observed.

The RO 25-9022 molecule has structural modifications that prevent it from being metabolized, therefore increasing its concentration in target cells and thus improving its bioactivity (Uskokovic *et al.*, 2001). The substitution of the C26 and C27 methyl with trifluoromethyl groups is one of the most significant side chain modifications that prevents hydroxylation at these positions and in this way significantly alters the susceptibility to metabolism, but as it turned out, it also facilitates the proton transfer effect.

The calculation of the free binding energy (score) of the RO 25-9022 molecule with redVDR allowed us to estimate its high affinity and attribute it to the proton transfer effect and thus to strong hydrogen bonding with His397 and His305. Such an interaction mechanism results not only in a high binding energy, but it can lead to qualitatively distinct VDR conformation and, together with the high metabolic stability of RO 25-9022 molecule, could be responsible for its high biological activity.

REFERENCES

Barthel TK, Mathern DR, Whitfield GK, Haussler CA, Andrew Hopper IV H, Hsieh J-C, Slater SA, Hsieh G, Kaczmarska M, Jurutka PW, Kolek OI, Ghishan FK, Haussler MR (2007) 1,25-dihydroxyvitamin D3/VDR-mediated induction of FGF23 as well as transcriptional control of other bone anabolic and catabolic genes that orchestrate the regulation of phosphate and calcium mineral metabolism. *J Steroid Biochem* **103:** 381–388.

Van den Bemd GJCM, Chang GTG (2002) Vitamin D and Vitamin D Analogs in Cancer Treatment. *Curr Drug Targets* **3**: 85–94.

Boyle BJ, Zhao XY, Cohen P, Feldman D (2001) Insulin-like growth factor binding protein-3 mediates 1 alpha,25-dihydroxyvitamin D3 growth inhibition in the LNCaP prostate cancer cell line through p21/WAF1. *J Urol* **165:** 1319–1324.

Brown AJ, Slatopolsky E (2008) Vitamin D analogs: Therapeutic applications and mechanisms for selectivity. *Mol Aspects Med* **29:** 433–452.

Cantorna MT, Hayes CE, DeLuca HF (1996) 1,25-Dihydroxyvitamin D3 reversibly blocks the progression of relapsing encephalomyelitis, a model of multiple sclerosis. *Proc Natl Acad Sci USA* **93:** 7861–7864.

Cantorna MT, Mahon BD (2004) Mounting Evidence for Vitamin D as an Environmental Factor Affecting Autoimmune Disease Prevalence. *Exp Biol Med* **229:** 1136–1142.

Chiang K-C, Chen TC (2009) Vitamin D for the prevention and treatment of pancreatic cancer. *World J Gastroenterol* **15:** 3349–3354.

Cornell WD, Cieplak P, Bayly CI, Gould IR, Merz KM Jr, Ferguson DM, Spellmeyer DC, Fox T, Caldwell JW, Kollman PA (1995) A 2nd generation force field for the simulation of proteins, nucleic acids and organic molecules. *J Am Chem Soc* **117:** 5179–5197.

Evans SR, Soldatenkov V, Shchepotin EB, Bogrash E, Shchepotin IB (1999) Novel 19-nor-hexafluoride vitamin D3 analog (Ro 25-6760) inhibits human colon cancer i*n vitro via* apoptosis. *Int J Oncol* 14: 979–985.

Fanfrlík J, Bronowska AK, Rezac J, Prenosil O, Konvalinka J, Hobza P (2010) A reliable docking/scoring scheme based on the semiempirical quantum mechanical PM6-DH2 method accurately covering dispersion and H-bonding: HIV-1 protease with 22 ligands. *J Phys Chem B* **114:** 12666–12678.

Fretz JA, Zella LA, Kim S, Shevde KN, Pike JW (2006) 1,25-Dihydroxyvitamin D3 regulates the expression of low-density lipoprotein receptor-related protein 5 *via* deoxyribonucleic acid sequence elements located downstream of the start site of transcription. *Mol Endocrinol* **20:** 2215–2230.

Gaschott T, Wachtershauser A, Steinhilber D, Stein J (2001) 1,25-Dihydroxycholecalciferol enhances butyrate-induced p21(Waf1/Cip1) expression. *Biochem Biophys Res Commun* 283: 80–85.

Guyton KZ, Kensler TW, Posner GH (2003) Vitamin D and vitamin D analogs as cancer chemopreventive agents. *Nutr Rev* **61:** 227–238.

Haussler MR, Haussler CA, Whitfield GK, Hsieh J-C, Thompson PD, Barthel TK, Bartik L, Egan JB, Wu Y, Kubicek JL, Lowmiller CL, Moffet EW, Forster RE, Jurutka PW (2010) The nuclear vitamin D receptor controls the expression of genes encoding factors which feed the "Fountain of Youth" to mediate healthful aging. *J Steroid Biochem Mol Biol* **121:** 88–97.

Haussler MR, Jurutka PW, Mizwicki M, Norman AW (2011) Vitamin D receptor (VDR)-mediated actions of 1α,25(OH)2vitamin D3: Genomic and non-genomic mechanisms. *Best Pract Res Cl En* **25:** 543–559.

Holick MT (2008) Vitamin D: a D-lightful health perspective. *Nutr Rev* **66:** S182–S194.

James SY, Mackay AG, Colston KW (1996) Effects of 1,25 dihydroxyvitamin D3 and its analogues on induction of apoptosis in breast cancer cells. *J Steroid Biochem Mol Biol* **58:** 395–401.

Kamel K, Kolinski A (2011) Computational study of binding of epothilone A to β-tubulin. *Acta Biochim Pol* **58:** 255–260.

Kawa S, Nikaido T, Aoki Y, Zhai Y, Kumagai T, Furihata K, Fujii S, Kiyosawa K (1997) Vitamin D analogues up-regulate p21 and p27 during growth inhibition of pancreatic cancer cell lines. *Br J Cancer* **76:** 884–889.

Klamt A, Schuurmann G (1993) COSMO — a new approach to dielectric screening in solvents with explicit expressions for the screening energy and its gradient. *J Chem Soc, Perkin Trans* **2:** 799–805.

Korth M, Pitonak M, Rezac J, Hobza P (2010) A transferable H-bonding correction for semiempirical quantum-chemical methods. *J Chem Theory Comput* **6:** 344–352.

Li P, Li C, Zhao X, Zhang X, Nicosia SV, Bai W (2004) p27(Kip1) stabilization and G(1) arrest by 1,25-dihydroxyvitamin D(3) in ovarian cancer cells mediated through down-regulation of cyclin E/cyclin-dependent kinase 2 and Skp1-Cullin-F-box protein/Skp2 ubiquitin ligase. *J Biol Chem* **279**: 25260–25267.

Malinen M, Saramaki A, Ropponen A, Degenhardt T, Vaisanen S, Carlberg C (2008) Distinct HDACs regulate the transcriptional response of human cyclin-dependent kinase inhibitor genes to Trichostatin A and 1alpha,25-dihydroxyvitamin D_3. *Nucleic Acids Res* **36**: 121–132.

Meyer MB, Watanuki M, Kim S, Shevde NK, Pike JW (2006) The human transient receptor potential vanilloid type 6 distal promoter contains multiple vitamin D receptor binding sites that mediate activation by 1,25-dihydroxyvitamin D_3 in intestinal cells. *Mol Endocrinol* **20:** 1447–1461.

Milat F, Ng KW (2009) Is Wnt signalling the final common pathway leading to bone formation? *Mol Cell Endocrinol* **310:** 52–62.

Moffatt KA, Johannes WU, Hedlund TE (2001) Growth inhibitory effects of 1a, 25-dihydroxyvitamin D_3 Are Mediated by Increased Levels of p21 in the Prostatic Carcinoma Cell Line ALVA-31. *Cancer Res* **61:** 7122–7129.

Morris GM, Goodsell DS, Halliday RS, Huey R, Hart J, Belew RK, Olson AJ (1998) Automated docking using a Lamarckian genetic algorithm and an empirical binding free energy function. *J Comput Chem* **19:** 1639–1662.

Narvaez CJ, Welsh J (1997) Differential effects of 1,25-dihydroxyvitamin D3 and tetradecanoylphorbol acetate on cell cycle and apoptosis of MCF-7 cells and a vitamin D_3-resistant variant. *Endocrinology* **138:** 4690–4698.

Nickeleit I, Zender S, Kossatz U, Malek NP (2007) $p27^{kip1}$: a target for tumor therapies? *Cell Div* **2:** 13.

Pettersen EF, Goddard TD, Huang CC, Couch GS, Greenblatt DM, Meng EC, Ferrin TE (2004) UCSF Chimera — a visualization system for exploratory research and analysis. *J Comput Chem* **25:** 1605–1612.

Raha K, Merz KM Jr (2005) Large-scale validation of a quantum mechanics based scoring function: predicting the binding affinity and the binding mode of a diverse set of protein-ligand complexes. *J Med Chem* **48:** 4558–4575.

Rochel N, Wurtz JM, Mitschler A, Klaholz B, Moras D (2000) The crystal structure of the nuclear receptor for vitamin D bound to its natural ligand. *Mol Cell* **5:** 173–179.

Schmidt MW, Baldridge KK, Boatz JA, Elbert ST, Gordon MS, Jensen JH, Koseki S, Matsunaga N, Nguyen KA, Su SJ, Windus TL, Dupuis M, Montgomery JA (1993) General atomic and molecular electronic structure system. *J Comput Chem* **14:** 1347–1363.

Schutz CN, Warshel A (2001) What are the dielectric "constants" of proteins and how to validate electrostatic models? *Proteins* **44:** 400–417.

Schwartz GG, Eads D, Naczki C, Northrup S, Chen T, Koumenis C (2008) 19-Nor-1 alpha,25-dihydroxyvitamin D2 (paricalcitol) inhibits the proliferation of human pancreatic cancer cells *in vitro* and *in vivo*. *Cancer Biol Ther* **7:** 430–436.

Singarapu KK, Zhu J, Tonelli M, Rao H, Assadi-Porter FM, Westler WM, DeLuca HF, Markley JL (2011) Ligand-specific structural changes in the vitamin D receptor in solution. *Biochemistry* **50:** 11025–11033.

Stewart JJP (2007) Optimization of parameters for semiempirical methods V: modification of NDDO approximations and application to 70 elements. *J Mol Model* **13:** 1173–1213.

Stewart JJP (2008) Stewart Computational Chemistry, Colorado Springs, CO, MOPAC2009; http://OpenMOPAC.net.

Stewart JJP (2009) Application of the PM6 method to modeling proteins. *J Mol Model* **15:** 765–805.

Swain CG, Unger SH, Rosenquist NR, Swain MS (1983) Substituent effects on chemical reactivity. improved evaluation of field and resonance components. *J Am Chem Soc* **105:** 492–502.

Tocchini-Valentini G, Rochel N, Wurtz JM, Mitschler A, Moras D (2001) Crystal structures of the vitamin D receptor complexed to superagonist 20-epi ligands. *P Natl Acad Sci USA* **98:** 5491–5496.

Tocchini-Valentini G, Rochel N, Wurtz JM, Moras D (2004) Crystal Structures of the Vitamin D Nuclear Receptor Liganded with the Vitamin D Side Chain Analogues Calcipotriol and Seocalcitol, Receptor Agonists of Clinical Importance. Insights into a Structural Basis for the Switching of Calcipotriol to a Receptor Antagonist by Further Side Chain Modification. *J Med Chem* **47:** 1956–1961.

Uskokovic MR, Norman AW, Manchand PS, Studzinski GP, Campbell MJ, Koeffler HP, Takeuchi A, Siu-Caldera M-L, Rao DS, Reddy GS (2001) Highly active analogs of 1a,25-dihydroxyvitamin D3 that resist metabolism through C-24 oxidation and C-3 epimerization pathways. *Steroids* **66:** 463–471.

Vaisanen S, Ryhanen S, Saarela JTA, Perakyla M, Andersin T, Maenpaa PH (2002) Structurally and functionally important amino acids of the agonistic conformation of the human Vitamin D receptor. *Mol Pharmacol* **62:** 788–794.

Wu G, Fan RS, Li W, Ko TC, Brattain MG (1997) Modulation of cell cycle control by vitamin D3 and its analogue, EB1089, in human breast cancer cells. *Oncogene* **15:** 1555–1563.

Zella JB, DeLuca HF (2003) Vitamin D and autoimmune diabetes. *J Cell Biochem* **88:** 216-222.

Zhuang S-H, Burnstein KR (1998) Antiproliferative effect of 1α,25-dihydroxyvitamin D_3 in human prostate cancer cell line LNCaP involves reduction of cyclin-dependent kinase 2 activity and persistent G1 accumulation. *Endocrinology* **139:** 1197–1207.